

# 1 Hexagonal modulation of theta rhythmic 2 attentional sampling of visual space

3 Ricardo Kienitz<sup>1,\*</sup>, Jan Martini<sup>2,3</sup> and Randolph F. Helfrich<sup>2,\*</sup>

4  
5 <sup>1</sup>*Goethe University Frankfurt, Epilepsy Center Frankfurt Rhine-Main, Department of Neurology,*  
6 *University Medicine Frankfurt, Schleusenweg 2-16, 60528 Frankfurt am Main, Germany*

7 <sup>2</sup>*Hertie Institute for Clinical Brain Research, Center for Neurology, University Medical Center Tübingen,*  
8 *Tübingen, Germany.*

9 <sup>3</sup>*International Max Planck Research School for the Mechanisms of Mental Function and Dysfunction,*  
10 *University of Tübingen, Tübingen, Germany*

11 \*Correspondence: ricardo.kienitz@med.uni-frankfurt.de and randolph.helfrich@gmail.com

12  
13  
14  
15 **Abbreviated title:** Hexagonal rhythmic attentional sampling

16  
17 **Conflict of interest:** The authors declare no competing conflict of interest.

18  
19 **Acknowledgements:** This work was supported by the German Research Foundation  
20 (HE8329/2-1 to RFH), the Medical Faculty of the University of Tübingen (JRG Plus  
21 program, RFH), the Hertie Foundation (Network for Excellence in Clinical  
22 Neuroscience; RFH), the Jung Foundation for Research and Science (Ernst Jung  
23 Career Advancement Award in Medicine; RFH) and the Medical Faculty of the  
24 University of Frankfurt (Clinician Scientist Program, RK).

25 **Author contributions:** Conceptualization: RK, RFH; Methodology: RK, JM, RFH;  
26 Formal Analysis: RK, JM; Investigation: JM; Resources: RFH; Writing – Original Draft,  
27 RK, RFH; Writing – Review & Editing: RK, JM, RFH; Supervision: RFH; Funding  
28 Acquisition: RFH.

30 **Summary**

31 Spatial attention improves visual perception by selecting behaviorally relevant sensory  
32 signals. Traditionally, attention has been conceptualized as a static spotlight, while  
33 recent evidence posited that attention operates as a moving spotlight that samples  
34 visual space sequentially in discrete snapshots that are clocked by theta rhythms (~3-  
35 8 Hz). While theta rhythmic attentional sampling has mainly been observed in fronto-  
36 parietal and occipital areas, theta oscillations also hallmark entorhinal-hippocampal  
37 grid-cell networks, which encode physical space in hexagonal patterns that guide overt  
38 exploration and navigation. We hypothesized that visual attention might rely on the  
39 same underlying principles and sample visual space in a hexagonal, grid-like  
40 configuration. To test this hypothesis, twenty participants performed a cue-guided  
41 attention task that probed behavioral performance as a function of space and time.  
42 Reaction times were assessed as a function of spatial location and varying cue-target  
43 intervals, which revealed prominent, spatially-structured theta rhythms. Specifically,  
44 higher theta power was evident at spatial locations that were aligned to multiples of  
45 60°, consistent with an underlying hexagonal organization. Participants that exhibited  
46 stronger hexagonal sampling relied less on the spatial cue to guide their attentional  
47 allocation. In sum, these findings suggest that covert visual attention relies on an  
48 underlying hexagonal grid-like structure known from the entorhinal-hippocampal  
49 system and highlight that theta rhythms reflect a common organizing principle for  
50 spatial cognition.

51

52 **Significance Statement**

53 Attention prioritizes sensory inputs to optimize behavior. But how does attention  
54 sample the environment in space and time? Here, we demonstrate that attentional  
55 sampling of visual space is not uniform, but preferentially explores locations that are  
56 oriented along a hexagonal pattern, reminiscent of the spatial configuration of  
57 entorhinal-hippocampal grid cells. Moreover, covert attentional sampling was clocked  
58 by theta oscillations (3-8 Hz). In sum, these findings provide evidence for a shared  
59 neural basis of underlying spatial attention and navigation and reveal that theta  
60 rhythms orchestrate sampling behaviors in space and time as a unifying principle  
61 underlying spatial cognition.

## 62 **Results**

63 Spatial attention prioritizes and selects behaviorally-relevant sensory signals to  
64 optimize visual perception that guides goal-directed behavior (Buschman & Kastner,  
65 2015). Traditionally, spatial attention has been conceptualized as a *static* spotlight that  
66 constantly amplifies visual input at a cued location. However, more recent theories  
67 suggest that attention might operate as a *moving* spotlight that samples and explores  
68 visual space sequentially (Fiebelkorn et al., 2013; Landau & Fries, 2012; VanRullen,  
69 2016). Critically, the sequential sampling of visual space does not occur randomly but  
70 is clocked by rhythmic brain activity. Converging evidence from behavior, (non-  
71 )invasive human and non-human primate electrophysiology studies jointly suggests  
72 that theta rhythms in the frontoparietal attention network and visual cortex orchestrate  
73 the rhythmic sampling of visual space (Fiebelkorn et al., 2018; Helfrich et al., 2018;  
74 Kienitz et al., 2018). Specifically, it had been proposed that alternating phases of theta  
75 oscillations provide distinct time windows to sample a spatial location and then shift  
76 attention to the next relevant location; hence, explaining why attention-guided visual  
77 perception is not static over time, but fluctuates as a function of the endogenous theta  
78 rhythms (Fiebelkorn & Kastner, 2019; Kienitz et al., 2022).

79 However, theta rhythmic behaviors are not confined to visual attention, but have  
80 been described in a variety of other sensory and cognitive modalities (Canolty &  
81 Knight, 2010; Colgin, 2013; Fries, 2023; Herweg et al., 2020; Lisman & Jensen, 2013).  
82 Theta oscillations are the most prominent electrophysiological signatures in the  
83 entorhinal-hippocampal system (Buzsáki, 2002, 2005) where their activity coordinates  
84 the firing of grid and place cells (Colgin, 2013; Moser et al., 2008). It has been firmly  
85 established that these cells represent the surrounding physical space and define a  
86 grid-like hexagonal pattern that facilitates orientation and navigation (Hafting et al.,  
87 2005; Moser et al., 2008). Similar to the theta rhythmic attentional sampling of the  
88 visual space, hippocampal theta sweeps might explore the surrounding physical space  
89 to identify the next navigational target to plan future movement trajectories (Vollan et  
90 al., 2024). Here we hypothesized that theta rhythmic attentional sampling might also  
91 sample space non-uniformly and preferentially explore locations that are oriented  
92 along an underlying spatial grid-like pattern that resembles the well-known  
93 hippocampal-entorhinal organization. Given the high degree of similarity between

94 theta-dependent behaviors in covert and overt exploration of space, we specifically  
95 tested if attention samples the visual environment in a grid-like, hexagonally-oriented  
96 pattern.

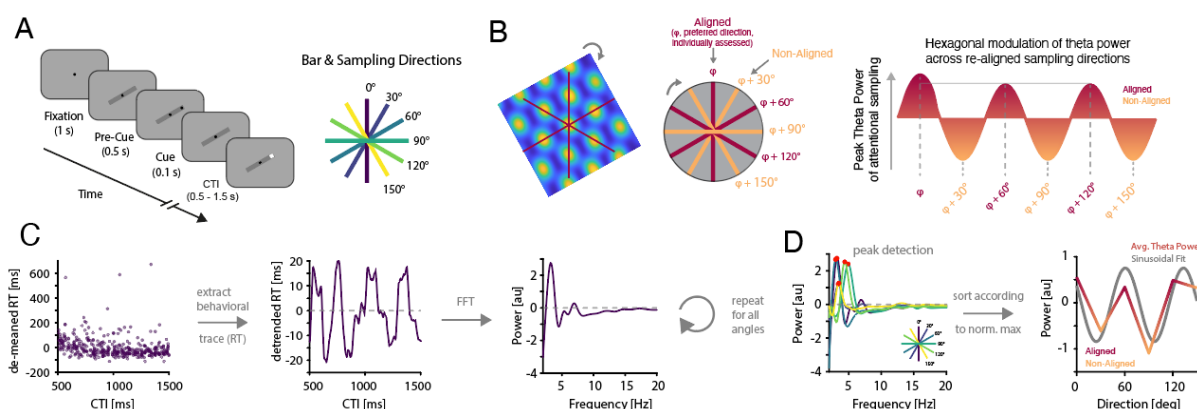
97 To probe whether the rhythmic attentional sampling of visual space follows a  
98 hexagonal modulation pattern, twenty participants performed a variant of a classic  
99 spatial attention task (Buschman & Kastner, 2015; Posner et al., 1980). On every trial,  
100 participants were presented with a bar that was oriented in one of six different  
101 directions (0-150° in steps of 30°; **Figure 1A**). After a delay, a spatial cue (90% validity)  
102 indicated the likely target position. The target stimulus was presented above  
103 perceptual threshold after a variable cue-target-interval (500-1500 ms). This design  
104 enabled resolving reaction times of target detection performance as a function of  
105 space and time. We predicted a hexagonal modulation of the resulting theta rhythmic  
106 sampling behavior with stronger sampling along the preferred cardinal axis  $\phi$  as well  
107 as at directions  $\phi$  plus integer multiples of 60° (**Figure 1B**). In contrast, we expected  
108 lower theta rhythmic sampling along non-aligned orientations, e.g.,  $\phi + 30^\circ$ .

109 As hypothesized, we observed a behavioral benefit at the cued location with  
110 significantly faster reaction times for cued than uncued targets ( $p = 0.03$ , Wilcoxon  
111 ranked sum test;  $294.9 \pm 8.1$  ms vs.  $307.9 \pm 7.3$  ms, mean  $\pm$  SEM, **Figure S1**). Grand-  
112 average reaction times did not differ significantly across the six different bar  
113 orientations ( $p = 0.99$ , RM-ANOVA, **Figure S1**). To resolve behavior as a function of  
114 space and time, we employed a moving window approach (window size: 50ms, step  
115 size: 1ms) to obtain a time-resolved estimate of reaction times. This approach was  
116 repeated for every bar orientation separately (**Figure 1C**). Subsequently, time-  
117 resolved behavioral estimates were spectrally decomposed after applying a Fast  
118 Fourier Transform (FFT). To assess theta power as a function of bar orientation, we  
119 detected the individual theta peak (peak in the range from 2.5-8 Hz) on the 1/f-  
120 corrected power spectra for all bar directions separately (**Figure 1D**). We observed an  
121 average theta peak frequency of  $4.6 \pm 0.1$  Hz across all participants (mean  $\pm$  SEM).  
122 The peak frequency did not differ significantly across the different bar orientations ( $p$   
123 = 0.11, one-way ANOVA).

124

125

[Figure 1]



126

### 127 Experimental design and approach

128 (A) Left: Participants performed a spatial attention task where they reacted to high-  
129 contrast target indicated an increase in luminance after having received a spatial cue (90 % validity) at  
130 either end of a bar. Different cue-target-intervals (CTI) allowed resolving reaction times as a function of  
131 time (as outlined in panel C). Right: The bar was randomly displayed at one of 6 possible main directions  
132 (right panel), allowing to assess attentional sampling along the 0, 30, 60, 90, 120 and 150° axes.

133 (B) The experimental design was geared towards assessing a hexagonal modulation of rhythmic  
134 attentional sampling. As entorhinal grid cell organization yields stronger activation in *aligned* directions  
135 (i.e., preferred direction  $\varphi$  as well as  $\varphi$  plus multiples of 60°) compared to *non-aligned* directions, we  
136 tested if attentional sampling along different directions also exhibits such a hexagonal modulation.

137 (C) Left: Single subject, single trial reaction times (demeaned). Center: Behavioral fluctuations were  
138 extracted from trials of a given orientation by binning and detrending reaction times across CTIs. Right:  
139 Time-resolved behavior was transformed to the frequency domain and power spectra were obtained  
140 per subject and bar orientation.

141 (D) Left: Individual peaks in the theta range (2.5–8 Hz) were then detected for each subject and angle  
142 on the 1/f corrected power spectra. The preferred individual direction  $\varphi$  was defined as the angle that  
143 exhibited the maximal theta power. Right: Angles were then re-aligned with respect to  $\varphi$ .

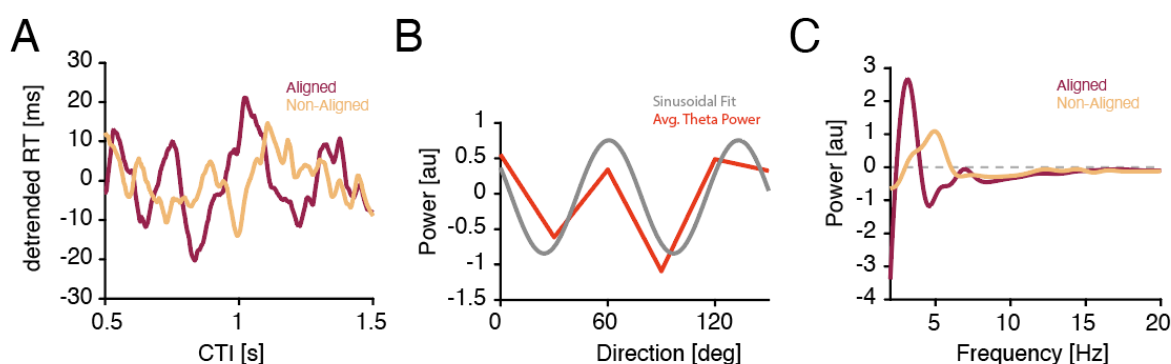
144

145 Our main hypothesis predicted that theta power should be modulated as a  
146 function of the precise bar orientation. Given that the preferred direction  $\varphi$  (i.e.  
147 direction with maximum theta power) differed across participants, we re-aligned the  
148 remaining orientations with respect to the preferred direction  $\varphi$  for each participant  
149 (analogous to (Doeller et al., 2010; Nau, Navarro Schröder, et al., 2018; Staudigl et  
150 al., 2018)). Relative to  $\varphi$ , the remaining orientations were grouped into *aligned* ( $\varphi$  plus  
151 multiples of 60°) and *non-aligned* directions. Note that we excluded  $\varphi$  from all  
152 subsequent analyses of *aligned* directions as the highest theta power defined  $\varphi$  and  
153 therefore, would have biased the subsequent results. We then collapsed behavioral  
154 estimates along the aligned and non-aligned orientations (Figure 2A). On the single  
155 subject level, a non-uniform distribution of theta peak power with higher power at  $\varphi$   
156 plus multiples of 60° was evident (Figure 2B/C).

157

158

**[Figure 2]**



159

160 **Single subject behavior**

161 (A) Average detrended reaction time traces for *aligned* (red) vs. *non-aligned* (orange) angles in one  
162 exemplary participant. Note the more pronounced fluctuations of reaction times for aligned angles.

163 (B) Theta peak power was non-uniformly distributed across the different angles. Higher power was  
164 found at the *aligned* (multiples of 60° with regard to  $\varphi$ ) compared to the *unaligned* directions, indicating  
165 a hexagonal modulation across angles.

166 (C) 1/f corrected power spectrum of the behavioral traces (*aligned* (red) vs. *non-aligned* (orange))  
167 directions. Note the higher power in the theta range for aligned directions. Results for this example  
168 subject implied a shift in peak frequency, which however was not present on the group level ( $p = 0.856$ ,  
169 Wilcoxon signed rank test).

170

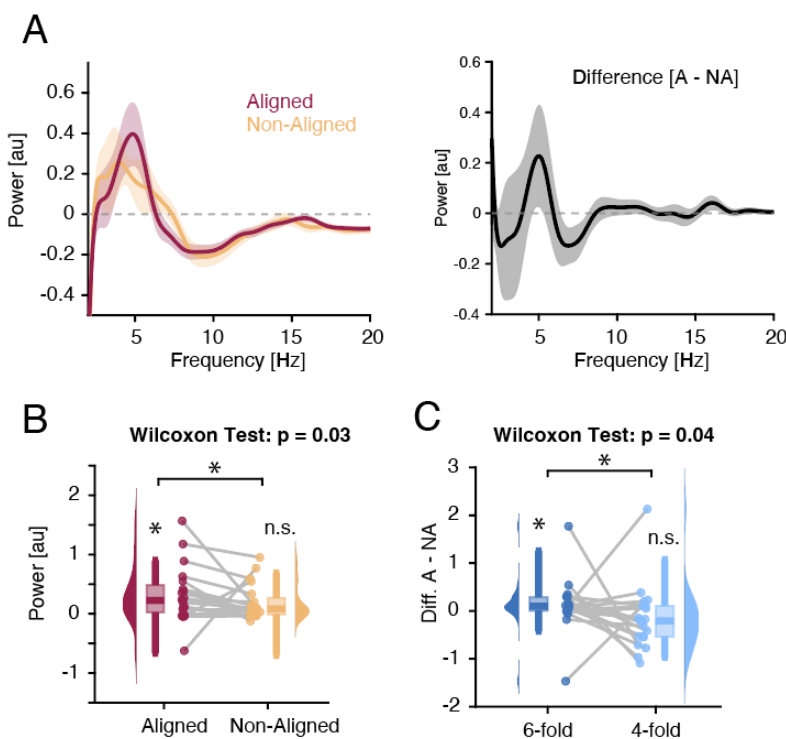
171 To quantify this observation at the group level, we repeated this analysis and  
172 alignment procedure for all participants. Across subjects, power values were non-  
173 uniformly distributed across angles ( $p = 9.54 \times 10^{-7}$ , sign-test across KL-divergences  
174 relative to uniform distributions). In the frequency domain, a clear theta peak for both,  
175 the *aligned* and *non-aligned* conditions was observed (Figure 3A). Yet, theta peak  
176 power significantly different between both conditions ( $p = 0.030$ , Wilcoxon signed rank  
177 test; Figure 3B), while peak frequency did not differ between both conditions ( $p =$   
178 0.856, Wilcoxon signed rank test). Critically, the theta power modulation was  
179 statistically significantly different from zero for the aligned ( $p = 0.021$ ), but not for the  
180 non-aligned condition ( $p = 0.057$ ). These results demonstrated that theta rhythmic  
181 sampling explored visual space non-uniformly with a preference for hexagonally  
182 oriented spatial locations.

183 As a control, we further tested if the observed effects were specific to a  
184 hexagonal (6-fold) modulation. Hence, we repeated the analysis on surrogate data  
185 that assumed a 4-fold modulation (Figure 3C; Methods). We observed a significantly  
186 stronger modulation in the 6-fold than 4-fold scenario ( $p = 0.043$ , Wilcoxon signed rank  
187 test). Critically, a significant modulation (as compared to 0) was observed for a 6-fold  
188 configuration ( $p = 0.008$ ), but not for the 4-fold configuration ( $p = 0.977$ ).

189

190

[Figure 3]



191

192

### Hexagonal modulation of attentional sampling

193

194

195

196

197

198

199

200

201

202

203

204

205

206

207

208

209

210

211

212

(A) Left: Grand-average 1/f-corrected power spectra for *aligned* (red) vs. *non-aligned* (orange) angles. Right: Power differences between aligned and non-aligned angles across participants. Note the peak in the theta range indicating higher theta power for aligned directions.

(B) Distributions of average theta power (4-6 Hz) for every participant for aligned (red,  $p = 0.021$ , Wilcoxon signed rank test) and non-aligned (orange,  $p = 0.057$ , Wilcoxon signed rank test) angles. Note the significantly higher average theta power for aligned angles ( $p = 0.030$ , Wilcoxon signed rank test).

(C) Distributions of modulation strength (*aligned* – *non-aligned* angles) for every participant for a 6-fold vs. 4-fold modulation. A significantly larger modulation was observed for the 6-fold modulation ( $p = 0.043$ , Wilcoxon signed rank test). Note that only the 6-fold modulation was significantly larger than zero ( $p(6fold>0) = 0.008$ ;  $p(4fold>0) = 0.977$ ).

203

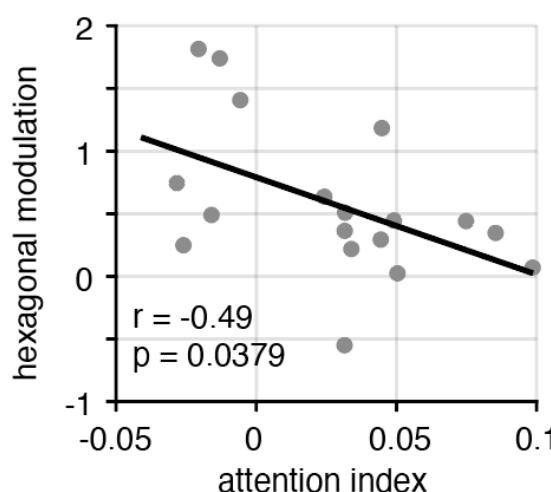
Finally, we explored whether hexagonal modulation mediates a behavioral advantage during allocation of spatial attention. Given that the hexagonal modulation provides a spatial framework for integrating information across visual space, we tested how individual hexagonal modulation of theta rhythmic sampling relates to attentional benefits of the spatial cue. Hence, we quantified the attention index as an established measure of attentional allocation (Fries et al., 2001) and assessed its relationship with the hexagonal modulation (difference in theta power between aligned and non-aligned orientations, cf. **Figure 3A**). Robust linear regression revealed a significant *negative* association between the attention index and hexagonal modulation (**Figure 4**,  $\beta = -$

213 7.76,  $p = 0.0379$ ,  $R^2 = 0.24$ ; linear correlation  $r = -0.49$ ), indicating that stronger  
214 hexagonal modulation is linked to a less pronounced benefit of spatial cue.

215

216

**[Figure 4]**



217

**218 Hexagonal modulation and attentional spatial cueing benefit**

219 Scatter plot illustrating the significant negative correlation ( $r = -0.49$ ) between the attention index (higher  
220 values indicate stronger benefits of the spatial attention cue) and hexagonal sampling (higher values  
221 indicate stronger hexagonal modulation of sampling).

222

223 Collectively, these results suggest that attention-guided visual target detection  
224 preferentially operates along an underlying hexagonal configuration that is oriented in  
225  $60^\circ$  steps, in accordance with a grid-like layout. Interestingly, rather than enhancing  
226 attentional benefits, stronger hexagonal modulation was associated with a reduced  
227 cueing effect; suggesting that individuals showing strong hexagonal sampling may  
228 sample visual space more extensively, and hence, rely less on a spatial attention cue.

229 **Discussion**

230 Here we demonstrate that *covert* attentional sampling of visual space is not uniformly  
231 organized, but follows an underlying hexagonal structure, which mimics the structure  
232 that defines the *overt* exploration of physical space known from entorhinal-  
233 hippocampal spatial coding. Analogous to the theta-dependent exploration of the  
234 environment, we observed theta rhythmic attentional sampling of visual space that  
235 was differentially modulated across different orientations adhering to a 6-fold  
236 hexagonal structure. Hence, these results demonstrate how attention samples the  
237 visual environment in space and time and provide a perspective how covert and overt  
238 behaviors might be linked through theta rhythmic interactions.

239

240 **Theta rhythms and attentional sampling**

241 Theta oscillations have been widely implicated in rhythmic attentional sampling,  
242 facilitating the sequential covert exploration of visual space (Fiebelkorn et al., 2013;  
243 Landau & Fries, 2012). This phenomenon spans multiple scales, from localized  
244 oscillatory activity (Kienitz et al., 2018) to large-scale network interactions in non-  
245 human primates and humans (Fiebelkorn et al., 2018; Helfrich et al., 2018). Consistent  
246 with this body of evidence, our results revealed robust theta rhythmicity in behavioral  
247 traces, evident as clear spectral peaks in the theta range in 1/f-corrected power  
248 spectra.

249 While previous studies established the temporal structure of rhythmic attentional  
250 sampling (Fiebelkorn & Kastner, 2019; Fries, 2023), we observed that this theta  
251 rhythmic modulation was not uniformly distributed across visual space. In the case of  
252 overt spatial exploration, it had been shown that entorhinal theta oscillations are a  
253 dominant signature and encode space in hexagonal pattern (Maidenbaum et al.,  
254 2018). These findings were recently extended by reports that overt exploration of  
255 *visual* space also show hexagonal modulations in humans (Staudigl et al., 2018).  
256 Hence, we predicted that theta oscillations might subserve a domain-general  
257 organizing principle of spatial and temporal cognition. In line with this prediction, our  
258 results revealed a non-uniform, hexagonal modulation of attentional sampling. This  
259 modulation of attentional sampling—a covert and cue-guided version of spatial  
260 exploration—is reminiscent of mechanisms that govern *overt* spatial exploration.

261 While spatial exploration has been studied in primates (Jutras et al., 2013; Killian et  
262 al., 2012) and humans (Doeller et al., 2010; Nau, Navarro Schröder, et al., 2018;  
263 Staudigl et al., 2018), much of the foundational work has been conducted in rodents,  
264 where place and grid cells in the entorhinal-hippocampal system are known to  
265 orchestrate navigational processes that are clocked by theta rhythms (Moser et al.,  
266 2008; O’Keefe, 1976). Moreover, recent studies in non-human primates and humans  
267 have demonstrated that grid-like signals in the entorhinal cortex can be triggered by  
268 covert spatial attention, independent of physical movement (Giari et al., 2023; Wilming  
269 et al., 2018). Our findings further substantiate this line of inquiry and demonstrate that  
270 rhythmic attentional sampling – a core principle of spatial attention – is modulated by  
271 an underlying hexagonal structure. These results suggest that rhythmic attentional  
272 sampling may rely on the same organizing principles that govern spatial exploration  
273 and navigation. In addition, our findings further imply that the observed hexagonal  
274 modulation is not a mere byproduct of rhythmic attentional sampling but may play an  
275 active role in shaping behavior. However, rather than enhancing attentional cueing  
276 benefits, stronger hexagonal modulation was associated with a reduced cueing effect,  
277 suggesting that individuals with more pronounced *intrinsic* hexagonal sampling may  
278 rely less on *extrinsic* spatial cues. This is in line with previous reports in non-human  
279 primates that demonstrated reduced neural theta oscillations in the visual cortex  
280 during focused attention (Spyropoulos et al., 2018). This raises the possibility that  
281 hexagonal modulation reflects an intrinsic spatial sampling mechanism that  
282 complements top-down attentional control.

283

#### 284 **A common neural basis for covert and overt behavior?**

285 It had long been speculated that attentional sampling relies on the same circuitry as  
286 overt behaviors as exemplified by the premotor theory (PMT) of attention (Rizzolatti et  
287 al., 1987). In line with a frontal origin, theta-dependent covert sampling has been  
288 observed in the frontal eye fields (FEF) as well as in adjacent frontal areas (Fiebelkorn  
289 et al., 2018; Helfrich et al., 2018; Raposo et al., 2023). Moreover, Gaillard et al.  
290 reported that saccadic eye movements are paced by a theta rhythm in FEF and  
291 explore space rhythmically (Gaillard et al., 2020). Given the prevalence of theta  
292 oscillations in fronto-parietal, occipital as well as entorhinal-hippocampal networks

293 during both covert sampling and overt spatial exploration, it is conceivable that their  
294 characteristics rely on shared neural mechanisms. To date, it remains unresolved  
295 whether the same mechanisms given rise to theta activity in archi- and neocortex.  
296 However, there is evidence that frontal and other regions' activity phase-lock to  
297 hippocampal theta rhythms during cognitive engagement (Hyman et al., 2005;  
298 Knudsen & Wallis, 2020; Sirota et al., 2008), thus, underscoring the notion that both  
299 are related.

300 Our results now provide additional behavioral evidence for a common neural basis.  
301 While theta rhythms likely originate from anatomically-distinct regions—such as the  
302 prefrontal and parietal attention network, occipital sensory areas and the entorhinal-  
303 hippocampal circuitry for navigation—they appear relevant for exploratory behaviors.  
304 Moreover, theta rhythms in different regions share several common features, such as  
305 phase coding (Kunz et al., 2019; Qasim et al., 2021; Smith et al., 2019), theta-gamma  
306 cross-frequency coupling (Canolty et al., 2006; Helfrich et al., 2018; Kienitz et al.,  
307 2021; Tort et al., 2009; Weber et al., 2024) or frequency modulation (Axmacher et al.,  
308 2010; Johnson et al., 2022) and are often reciprocally coupled (Daume et al., 2024;  
309 Johnson et al., 2023; Tamura et al., 2017). Hence, it is conceivable that theta-coupled  
310 behaviors constitute a unifying framework for spatial cognition. This consideration  
311 entails that the geometric hexagonal organization might not only subserve spatial  
312 maps, but could potentially also structure cognitive maps (Constantinescu et al., 2016;  
313 Epstein et al., 2017; Nau, Julian, et al., 2018), thus, reflecting a core principle  
314 underlying human cognition.

315

## 316 **Limitations and Future Directions**

317 In the present study, we observed clear theta rhythmic sampling behavior. Critically,  
318 theta rhythmicity was modulated as a function of space. While our study provides  
319 behavioral evidence for hexagonal modulation of covert attentional sampling, several  
320 limitations need be acknowledged. First, only behavioral data was acquired, thus, we  
321 cannot resolve the putative neuroanatomical origins of the observed rhythms. It is  
322 likely that an interplay between frontoparietal attention networks, visual areas and  
323 hippocampal-prefrontal networks forms the basis for theta rhythmic sampling  
324 (Fiebelkorn & Kastner, 2019; Kienitz et al., 2022). However, previous work also

325 implicated the thalamus in orchestrating theta-dependent network (Fiebelkorn et al.,  
326 2019; Griffiths et al., 2022; Sweeney-Reed et al., 2015). Hence, future studies that  
327 employ simultaneous, high spatiotemporal recordings from the different network  
328 nodes, ideally by means of intracranial electroencephalography (Parvizi & Kastner,  
329 2018), need to determine whether covert and overt sampling behaviors indeed rely on  
330 the same underlying neural mechanisms.

331 Secondly, theta rhythmicity has been contested recently. Especially potentially  
332 inappropriate surrogate testing has been identified as a source of potential bias that  
333 disrupts inherent signal autocorrelations (Brookshire, 2022; Fiebelkorn, 2022; Re et  
334 al., 2022; Tosato et al., 2022). Here, we did not employ time-shuffled surrogate testing,  
335 but instead employed within-subject comparisons across different sampling  
336 orientations. We observed that spectral differences between aligned and non-aligned  
337 conditions peaked in the theta range (~5 Hz). This is in line with recent lesion work  
338 that demonstrated that a focal disruption of the frontoparietal attention network alters  
339 theta rhythmic attentional sampling (Raposo et al., 2023).

340 Third, the employed paradigm was designed to test a specific hypothesis and thus,  
341 focused specifically on a 6-fold modulation and testing it against a 4-fold modulation  
342 pattern. Although the results support a hexagonal organization, other spatial  
343 configurations cannot be entirely ruled out. While we recorded a high trial count per  
344 participants (3000 trials across two sessions, which exceeds typically reported trial  
345 numbers, cf. (Fiebelkorn et al., 2013; Helfrich et al., 2018; Landau & Fries, 2012)) to  
346 detect subtle rhythmic effects, incorporating additional trials and spatial orientations  
347 proved challenging, since it rendered the experiment unacceptably long (> 3-4h).

348 Lastly, we did not include the optimal direction into our ‘aligned’ condition.  
349 Furthermore, we equated the number of angles for the ‘aligned’ and ‘non-aligned’  
350 conditions to mitigate any sampling bias. While this is considered best practice, it  
351 needs to be stressed that omitting the optimal phase also attenuates the overall effect  
352 size.

353

## 354 **Conclusion**

355 Collectively, our findings demonstrate that visual attention samples visual space along  
356 an underlying hexagonal grid-like layout. This non-uniform sampling of visual space

357 was clocked by theta rhythmic activity. Hence, these results provide a perspective how  
358 the brain might employ similar mechanisms to support both, covert and overt  
359 exploratory behaviors, and extends known spatio-temporal coding mechanisms during  
360 spatial exploration to covert attentional processing. In sum, this study demonstrates  
361 how the brain samples the visual environment in space and time, with theta oscillations  
362 reflecting a unifying principle underlying spatial cognition.

363 **Materials and Methods**

364 *Participants*

365 20 adults ( $26.15 \pm 4.07$  years; mean  $\pm$  SD; 10 females) participated in the study. The  
366 study and analyses were approved by the IRB board at the University Medical Center  
367 Tübingen (protocol number 049/2020BO2) in accordance with the Declaration of  
368 Helsinki. All participants provided informed written consent to participate in the study.

369

370 *Experimental design and procedures*

371 Each trial began with the presentation of a central fixation point (0.7° visual angle)  
372 displayed for 500 ms to maintain participants' visual attention. Following the fixation,  
373 a central bar, subtending 5° of visual angle, appeared for another 500 ms. The  
374 orientation of the bar was randomly chosen from 12 primary directions, equally spaced  
375 around a circle (e.g., 0°, 30°, 60°, ..., 330°). After the bar presentation, a brief  
376 peripheral spatial cue, 0.7° in visual angle, was displayed for 100 ms to indicate the  
377 location where the target was most likely to appear (cue-validity of 90%). After the cue,  
378 a variable cue-target interval (500–1500 ms; CTI) was introduced. This interval was  
379 divided into 25 equal bins, with the target appearing randomly in one of these bins  
380 within each trial. The target, which subtended 0.7° of visual angle, was presented as  
381 a brief flash lasting only 17 ms. Participants were instructed to respond as quickly as  
382 possible to the target by pressing a designated key, with a response deadline of 1  
383 second after target presentation. Responses made prematurely during the cue-target  
384 interval were recorded but marked as invalid. On 5% of trials (catch trials), no target  
385 was presented to ensure participants remained attentive to the task.

386 The experiment was conducted over two sessions on separate days, with each  
387 session comprising 1,500 trials, divided into 15 blocks of 100 trials each. Each of the  
388 12 bar orientations was presented equally across trials, ensuring balanced sampling.  
389 Stimuli were generated using MATLAB (The MathWorks, Natick, MA) and the  
390 Psychophysics Toolbox and were presented on a calibrated display at an approximate  
391 viewing distance of 70 cm. Visual angles were computed based on screen dimensions  
392 and viewing distance.

393

394

395 *Cue Validity Effect on Reaction Times*

396 To evaluate the influence of cue validity on reaction times, behavioral data were  
397 preprocessed to exclude outliers identified using Cook's distance. Reaction times for  
398 valid (cue predicted target location) and invalid (cue did not predict target location)  
399 trials were averaged across participants. A Wilcoxon signed-rank test was employed  
400 to determine statistical differences between valid and invalid conditions, testing the  
401 hypothesis that valid cues yield faster reaction times.

402

403 *Reaction Time Across Target Angles*

404 The relationship between reaction times and target angles was assessed by grouping  
405 trials based on bar orientation angles. For each participant, outliers (determined using  
406 Cook's distance) and trials with invalid cues were excluded. Reaction times were  
407 averaged for each angle, including the angle's counter-angle (e.g., 0° and 180°). A  
408 repeated-measures analysis of variance (RM-ANOVA) tested whether reaction times  
409 differed significantly across target angles.

410

411 *Extraction of the behavioral reaction time trace*

412 To investigate temporal dynamics of attentional sampling, reaction time traces were  
413 computed for each participant across experimental conditions. Outliers were identified  
414 using Cook's distance and removed alongside trials with invalid cues. For each  
415 participant, trials were grouped based on bar orientation angles, where each angle  
416 was paired with its counter-angle (e.g., 0° and 180°). Time-resolved behavioral traces  
417 were derived using a 50 ms sliding window moving in 1 ms steps, smoothed with a 25  
418 ms window to interpolate any remaining values that resulted from the limited temporal  
419 sampling, and were aligned to the cue-target interval. Condition-specific traces were  
420 computed for each bar orientation. Time vectors were normalized to align with the CTI  
421 range and expressed in seconds for subsequent analyses.

422

423 *Spectral analysis of reaction time traces*

424 To explore rhythmic components in reaction time data, behavioral traces were  
425 transformed into the frequency domain. To this end, we applied the Fast Fourier  
426 Transform (FFT) on preprocessed RT traces from all participants and conditions to

427 compute power spectra for each condition and participant. Power spectra were  
428 calculated separately for all bar orientations and aggregated across trials. To correct  
429 for the aperiodic component in the power spectra, a power-law function was fitted to  
430 the frequency distribution of each spectrum, and the resulting 1/f background  
431 removed. Following spectral decomposition, grand-averaged power spectra were  
432 computed for each condition.

433 To investigate theta rhythmic dynamics of attentional sampling, peak frequencies and  
434 corresponding power values were extracted from the frequency-domain reaction time  
435 data. For each orientation, local maxima in the power spectrum were identified within  
436 the theta range (2.5 – 8 Hz) to determine the peak frequency and its associated power.  
437 If no clear peak was detected, the maximum power within the theta range was  
438 selected. To account for baseline fluctuations, power spectra were detrended,  
439 ensuring that periodic rhythmic activity was isolated.

440 Non-uniformity of power values across angles was computed as the Kullback-Leibler  
441 (KL) divergence between each subject's observed power distribution and a uniform  
442 distribution, with a value of zero indicating no difference. We then performed a one-  
443 tailed nonparametric sign test across subjects testing whether the observed KL-  
444 divergences were systematically greater than zero. Each participant's preferred  
445 orientation was defined as the angle with the highest detrended theta power ( $\varphi$ ). Power  
446 and frequency values for all other orientations were then realigned relative to  $\varphi$ . Mean  
447 peak frequencies were calculated for each bar orientation, and a one-way analysis of  
448 variance (ANOVA) was conducted to test whether peak frequencies differed  
449 significantly across orientations.

450 To examine the spatial organization of theta rhythmicity in attentional sampling, power  
451 spectra were compared between bar orientations aligned and non-aligned to  $\varphi$ .  
452 Aligned and non-aligned angles were grouped according to a 6-fold modulation pattern  
453 (spaced by 60°), reflecting the hypothesized hexagonal organization of attentional  
454 sampling. For each participant, power spectra were averaged across aligned and non-  
455 aligned orientations, respectively. The preferred angle  $\varphi$  was excluded to avoid bias  
456 and number of angles was matched to avoid sampling bias. Power differences  
457 between aligned and non-aligned orientations were calculated around the prominent  
458 peak in theta frequency range (4–6 Hz, **Figure 3A**). Control analyses examined the

459 specificity of the observed 6-fold modulation by comparing it with a 4-fold modulation  
460 pattern (spaced by 90°). A Wilcoxon signed-rank test was used to assess statistical  
461 differences in theta power between aligned and non-aligned conditions.

462 To examine how hexagonal modulation relates to attentional performance, we  
463 computed the attention modulation index (Fries et al., 2001), which quantifies the  
464 behavioral benefit of valid versus invalid cues. The attention index was calculated as:

465

466 
$$\text{attention index} = \frac{RT_{invalid} - RT_{valid}}{RT_{invalid} + RT_{valid}}$$

467

468 where  $RT_{valid}$  and  $RT_{invalid}$  represent the mean reaction times (RTs) for valid and  
469 invalid cues, respectively. A higher attention index reflects stronger attentional  
470 benefits, as it corresponds to a greater reduction in RTs for validly cued trials relative  
471 to invalidly cued trials. Hexagonal modulation was defined as the difference in theta  
472 power between aligned and non-aligned orientations (in a 6-fold modulation pattern)  
473 in the 4-6 Hz frequency range (cf. **Figure 3A**). We applied robust linear regression to  
474 assess the relationship between these two measures, identifying and excluding  
475 outliers using Cook's distance (2 participants).

476 **References**

477 Axmacher, N., Henseler, M. M., Jensen, O., Weinreich, I., Elger, C. E., & Fell, J.  
478 (2010). Cross-frequency coupling supports multi-item working memory in the  
479 human hippocampus. *Proceedings of the National Academy of Sciences of the*  
480 *United States of America*, 107(7), 3228–3233.  
481 <https://doi.org/10.1073/pnas.0911531107>

482 Brookshire, G. (2022). Putative rhythms in attentional switching can be explained by  
483 aperiodic temporal structure. *Nature Human Behaviour*, 6(9), 1280–1291.  
484 <https://doi.org/10.1038/s41562-022-01364-0>

485 Buschman, T. J., & Kastner, S. (2015). From Behavior to Neural Dynamics: An  
486 Integrated Theory of Attention. *Neuron*, 88(1), 127–144.  
487 <https://doi.org/10.1016/j.neuron.2015.09.017>

488 Buzsáki, G. (2002). Theta oscillations in the hippocampus. *Neuron*, 33(3), 325–340.  
489 [https://doi.org/10.1016/S0896-6273\(02\)00586-X](https://doi.org/10.1016/S0896-6273(02)00586-X)

490 Buzsáki, G. (2005). Theta rhythm of navigation: Link between path integration and  
491 landmark navigation, episodic and semantic memory. *Hippocampus*, 15(7),  
492 827–840. <https://doi.org/10.1002/hipo.20113>

493 Canolty, R. T., Edwards, E., Dalal, S. S., Soltani, M., Nagarajan, S. S., Kirsch, H. E.,  
494 Berger, M. S., Barbaro, N. M., & Knight, R. T. (2006). High gamma power is  
495 phase-locked to theta oscillations in human neocortex. *Science (New York,*  
496 *N.Y.)*, 313, 1626–1628. <https://doi.org/10.1126/science.1128115>

497 Canolty, R. T., & Knight, R. T. (2010). The functional role of cross-frequency coupling.  
498 *Trends in Cognitive Sciences*, 14(11), 506–515.  
499 <https://doi.org/10.1016/j.tics.2010.09.001>

500 Colgin, L. L. (2013). Mechanisms and functions of theta rhythms. *Annual Review of*  
501 *Neuroscience*, 36, 295–312. <https://doi.org/10.1146/annurev-neuro-062012-170330>

503 Constantinescu, A. O., O'Reilly, J. X., & Behrens, T. E. J. (2016). Organizing  
504 conceptual knowledge in humans with a gridlike code. *Science*, 352(6292).  
505 <https://doi.org/10.1126/science.aaf0941>

506 Daume, J., Kamiński, J., Schjetnan, A. G. P., Salimpour, Y., Khan, U., Kyzar, M., Reed,  
507 C. M., Anderson, W. S., Valiante, T. A., Mamelak, A. N., & Rutishauser, U.  
508 (2024). Control of working memory by phase–amplitude coupling of human  
509 hippocampal neurons. *Nature*, 629(8011), 393–401.  
510 <https://doi.org/10.1038/s41586-024-07309-z>

511 Doeller, C. F., Barry, C., & Burgess, N. (2010). Evidence for grid cells in a human  
512 memory network. *Nature*, 463(7281), 657–661.  
513 <https://doi.org/10.1038/nature08704>

514 Epstein, R. A., Patai, E. Z., Julian, J. B., & Spiers, H. J. (2017). The cognitive map in  
515 humans: Spatial navigation and beyond. *Nature Neuroscience*, 20(11), 1504–  
516 1513. <https://doi.org/10.1038/nn.4656>

517 Fiebelkorn, I. C. (2022). There Is More Evidence of Rhythmic Attention than Can Be  
518 Found in Behavioral Studies: Perspective on Brookshire, 2022. *Journal of*  
519 *Cognitive Neuroscience*, 35(1), 128–134.  
520 [https://doi.org/10.1162/jocn\\_a\\_01936](https://doi.org/10.1162/jocn_a_01936)

521 Fiebelkorn, I. C., & Kastner, S. (2019). A Rhythmic Theory of Attention. *Trends in*  
522 *Cognitive Sciences*, 23(2), 87–101. <https://doi.org/10.1016/j.tics.2018.11.009>

523 Fiebelkorn, I. C., Pinsk, M. A., & Kastner, S. (2018). A Dynamic Interplay within the  
524 Frontoparietal Network Underlies Rhythmic Spatial Attention. *Neuron*, 99(4),  
525 842-853.e8. <https://doi.org/10.1016/j.neuron.2018.07.038>

526 Fiebelkorn, I. C., Pinsk, M. A., & Kastner, S. (2019). The mediodorsal pulvinar  
527 coordinates the macaque fronto-parietal network during rhythmic spatial  
528 attention. *Nature Communications*, 10(1), 215.

529 Fiebelkorn, I. C., Saalmann, Y. B., & Kastner, S. (2013). Rhythmic sampling within and  
530 between objects despite sustained attention at a cued location. *Current*  
531 *Biology: CB*, 23(24), 2553–2558. <https://doi.org/10.1016/j.cub.2013.10.063>

532 Fries, P. (2023). Rhythmic attentional scanning. *Neuron*, 111(7), 954–970.  
533 <https://doi.org/10.1016/j.neuron.2023.02.015>

534 Fries, P., Reynolds, J. H., Rorie, A. E., & Desimone, R. (2001). Modulation of  
535 oscillatory neuronal synchronization by selective visual attention. *Science (New*  
536 *York, N.Y.)*, 291(5508), 1560–1563.  
537 <https://doi.org/10.1126/science.291.5508.1560>

538 Gaillard, C., Ben Hadj Hassen, S., Di Bello, F., Bihan-Poudec, Y., VanRullen, R., &  
539 Ben Hamed, S. (2020). Prefrontal attentional saccades explore space  
540 rhythmically. *Nature Communications*, 11(1), 1–13.  
541 <https://doi.org/10.1038/s41467-020-14649-7>

542 Giari, G., Vignali, L., Xu, Y., & Bottini, R. (2023). MEG frequency tagging reveals a  
543 grid-like code during covert attentional movements. *Cell Reports*.  
544 <https://doi.org/10.1016/j.celrep.2023.113209>

545 Griffiths, B. J., Zaehle, T., Repplinger, S., Schmitt, F. C., Voges, J., Hanslmayr, S., &  
546 Staudigl, T. (2022). Rhythmic interactions between the mediodorsal thalamus  
547 and prefrontal cortex precede human visual perception. *Nature Communications*, 13(1), 3736. <https://doi.org/10.1038/s41467-022-31407-z>

549 Hafting, T., Fyhn, M., Molden, S., Moser, M. B., & Moser, E. I. (2005). Microstructure  
550 of a spatial map in the entorhinal cortex. *Nature*, 436(7052), 801–806.  
551 <https://doi.org/10.1038/nature03721>

552 Helfrich, R. F., Fiebelkorn, I. C., Szczepanski, S. M., Lin, J. J., Parvizi, J., Knight, R.  
553 T., & Kastner, S. (2018). Neural Mechanisms of Sustained Attention Are  
554 Rhythmic. *Neuron*, 99(4), 854–865.  
555 <https://doi.org/10.1016/j.neuron.2018.07.032>

556 Herweg, N. A., Solomon, E. A., & Kahana, M. J. (2020). Theta Oscillations in Human  
557 Memory. *Trends in Cognitive Sciences*, 24(3), 208–227.  
558 <https://doi.org/10.1016/j.tics.2019.12.006>

559 Hyman, J. M., Zilli, E. A., Paley, A. M., & Hasselmo, M. E. (2005). Medial prefrontal  
560 cortex cells show dynamic modulation with the hippocampal theta rhythm  
561 dependent on behavior. *Hippocampus*, 15(6), 739–749.  
562 <https://doi.org/10.1002/hipo.20106>

563 Johnson, E. L., Lin, J. J., King-Stephens, D., Weber, P. B., Laxer, K. D., Saez, I.,  
564 Girgis, F., D'Esposito, M., Knight, R. T., & Badre, D. (2023). A rapid theta

565 network mechanism for flexible information encoding. *Nature Communications*,  
566 14(1), 2872. <https://doi.org/10.1038/s41467-023-38574-7>

567 Johnson, E. L., Yin, Q., O'Hara, N. B., Tang, L., Jeong, J.-W., Asano, E., & Ofen, N.  
568 (2022). Dissociable oscillatory theta signatures of memory formation in the  
569 developing brain. *Current Biology*, 32(7), 1457-1469.e4.  
570 <https://doi.org/10.1016/j.cub.2022.01.053>

571 Jutras, M. J., Fries, P., & Buffalo, E. a. (2013). Oscillatory activity in the monkey  
572 hippocampus during visual exploration and memory formation. *Proceedings of  
573 the National Academy of Sciences*, 110(32), 13144–13149.  
574 <https://doi.org/10.1073/pnas.1302351110/>  
575 /DCSupplemental.www.pnas.org/cgi/doi/10.1073/pnas.1302351110

576 Kienitz, R., Cox, M. A., Dougherty, K., Saunders, R. C., Schmiedt, J. T., Leopold, D.  
577 A., Maier, A., & Schmid, M. C. (2021). Theta, but Not Gamma Oscillations in  
578 Area V4 Depend on Input from Primary Visual Cortex. *Current Biology*, 31(3),  
579 635-642.e3. <https://doi.org/10.1016/j.cub.2020.10.091>

580 Kienitz, R., Schmid, M. C., & Dugué, L. (2022). Rhythmic sampling revisited:  
581 Experimental paradigms and neural mechanisms. *European Journal of  
582 Neuroscience*, 1–15. <https://doi.org/10.1111/ejn.15489>

583 Kienitz, R., Schmiedt, J. T., Shapcott, K. A., Kouroupaki, K., Saunders, R. C., &  
584 Schmid, M. C. (2018). Theta Rhythmic Neuronal Activity and Reaction Times  
585 Arising from Cortical Receptive Field Interactions during Distributed Attention.  
586 *Current Biology*, 1–11. <https://doi.org/10.1016/j.cub.2018.05.086>

587 Killian, N. J., Jutras, M. J., & Buffalo, E. a. (2012). A map of visual space in the primate  
588 entorhinal cortex. *Nature*, 491(7426), 761–764.  
589 <https://doi.org/10.1038/nature11587>

590 Knudsen, E. B., & Wallis, J. D. (2020). Closed-Loop Theta Stimulation in the  
591 Orbitofrontal Cortex Prevents Reward-Based Learning. *Neuron*, 106(3), 537-  
592 547.e4. <https://doi.org/10.1016/j.neuron.2020.02.003>

593 Kunz, L., Wang, L., Lachner-Piza, D., Zhang, H., Brandt, A., Dümpelmann, M.,  
594 Reinacher, P. C., Coenen, V. A., Chen, D., Wang, W.-X., Zhou, W., Liang, S.,  
595 Grawe, P., Bien, C. G., Bierbrauer, A., Navarro Schröder, T., Schulze-Bonhage,  
596 A., & Axmacher, N. (2019). Hippocampal theta phases organize the reactivation  
597 of large-scale electrophysiological representations during goal-directed  
598 navigation. *Science Advances*, 5(7), eaav8192.  
599 <https://doi.org/10.1126/sciadv.aav8192>

600 Landau, A. N., & Fries, P. (2012). Attention samples stimuli rhythmically. *Current  
601 Biology: CB*, 22(11), 1000–1004. <https://doi.org/10.1016/j.cub.2012.03.054>

602 Lisman, J. E., & Jensen, O. (2013). The Theta-Gamma neural code. *Neuron*, 77(6),  
603 1002–1016. <https://doi.org/10.1016/j.neuron.2013.03.007>

604 Maidenbaum, S., Miller, J., Stein, J. M., & Jacobs, J. (2018). Grid-like hexadirectional  
605 modulation of human entorhinal theta oscillations. *Proceedings of the National  
606 Academy of Sciences*, 201805007. <https://doi.org/10.1073/pnas.1805007115>

607 Moser, E. I., Kropff, E., & Moser, M. B. (2008). Place cells, grid cells, and the brain's  
608 spatial representation system. *Annual Review of Neuroscience*, 31, 69–89.  
609 <https://doi.org/10.1146/annurev.neuro.31.061307.090723>

610 Nau, M., Julian, J. B., & Doeller, C. F. (2018). How the Brain's Navigation System  
611 Shapes Our Visual Experience. *Trends in Cognitive Sciences*, 22(9), 810–825.  
612 <https://doi.org/10.1016/j.tics.2018.06.008>

613 Nau, M., Navarro Schröder, T., Bellmund, J. L. S., & Doeller, C. F. (2018).  
614 Hexadirectional coding of visual space in human entorhinal cortex. *Nature  
615 Neuroscience*, 21(2), 188–190. <https://doi.org/10.1038/s41593-017-0050-8>

616 O'Keefe, J. (1976). Place units in the hippocampus of the freely moving rat.  
617 *Experimental Neurology*, 51(1), 78–109. [https://doi.org/10.1016/0014-4886\(76\)90055-8](https://doi.org/10.1016/0014-<br/>618 4886(76)90055-8)

619 Parvizi, J., & Kastner, S. (2018). Promises and limitations of human intracranial  
620 electroencephalography. *Nature Neuroscience*, 21(April).  
621 <https://doi.org/10.1038/s41593-018-0108-2>

622 Posner, M. I., Snyder, C. R. R., & Davidson, B. J. (1980). Attention and the detection  
623 of signals. *Journal of Experimental Psychology: General*, 109(2), 160–174.  
624 <https://doi.org/10.1111/j.1755-6724.1986.mp60004004.x>

625 Qasim, S. E., Fried, I., & Jacobs, J. (2021). Phase precession in the human  
626 hippocampus and entorhinal cortex. *Cell*, 184(12), 3242-3255.e10.  
627 <https://doi.org/10.1016/j.cell.2021.04.017>

628 Raposo, I., Szczepanski, S. M., Haaland, K., Endestad, T., Solbakk, A.-K., Knight, R.  
629 T., & Helfrich, R. F. (2023). Periodic attention deficits after frontoparietal lesions  
630 provide causal evidence for rhythmic attentional sampling. *Current Biology*,  
631 33(22), 4893-4904.e3. <https://doi.org/10.1016/j.cub.2023.09.065>

632 Re, D., Tosato, T., Fries, P., & Landau, A. N. (2022). *Perplexity about periodicity  
633 repeats perpetually: A response to Brookshire* (p. 2022.09.26.509017). bioRxiv.  
634 <https://doi.org/10.1101/2022.09.26.509017>

635 Rizzolatti, G., Riggio, L., Dascola, I., & Umiltá, C. (1987). Reorienting attention across  
636 the horizontal and vertical meridians: Evidence in favor of a premotor theory of  
637 attention. *Neuropsychologia*, 25(1A), 31–40. [https://doi.org/10.1016/0028-3932\(87\)90041-8](https://doi.org/10.1016/0028-<br/>638 3932(87)90041-8)

639 Sirota, A., Montgomery, S., Fujisawa, S., Isomura, Y., Zugaro, M., & Buzsáki, G.  
640 (2008). Entrainment of neocortical neurons and gamma oscillations by the  
641 hippocampal theta rhythm. *Neuron*, 60(4), 683–697.  
642 <https://doi.org/10.1016/j.neuron.2008.09.014>

643 Smith, E. H., Horga, G., Yates, M. J., Mikell, C. B., Banks, G. P., Pathak, Y. J.,  
644 Schevon, C. A., McKhann, G. M., Hayden, B. Y., Botvinick, M. M., & Sheth, S.  
645 A. (2019). Widespread temporal coding of cognitive control in the human  
646 prefrontal cortex. *Nature Neuroscience*, 22(11), 1883–1891.  
647 <https://doi.org/10.1038/s41593-019-0494-0>

648 Spyropoulos, G., Bosman, C. A., & Fries, P. (2018). A theta rhythm in macaque visual  
649 cortex and its attentional modulation. *Proceedings of the National Academy of  
650 Sciences*, 115(24), E5614–E5623. <https://doi.org/10.1073/pnas.1719433115>

651 Staudigl, T., Leszczynski, M., Jacobs, J., Sheth, S. A., Schroeder, C. E., Jensen, O.,  
652 & Doeller, C. F. (2018). Hexadirectional Modulation of High-Frequency  
653 Electrophysiological Activity in the Human Anterior Medial Temporal Lobe

654 Maps Visual Space. *Current Biology*, 28(20), 3325-3329.e4.  
655 <https://doi.org/10.1016/j.cub.2018.09.035>

656 Sweeney-Reed, C. M., Zaehle, T., Voges, J., Schmitt, F. C., Buentjen, L., Kopitzki, K.,  
657 Hinrichs, H., Heinze, H.-J., Rugg, M. D., Knight, R. T., & Richardson-Klavehn,  
658 A. (2015). Thalamic theta phase alignment predicts human memory formation  
659 and anterior thalamic cross-frequency coupling. *eLife*, 4, e07578.  
660 <https://doi.org/10.7554/eLife.07578>

661 Tamura, M., Spellman, T. J., Rosen, A. M., Gogos, J. A., & Gordon, J. A. (2017).  
662 Hippocampal-prefrontal theta-gamma coupling during performance of a spatial  
663 working memory task. *Nature Communications*, 8(1), 2182.  
664 <https://doi.org/10.1038/s41467-017-02108-9>

665 Tort, A. B. L., Komorowski, R. W., Manns, J. R., Kopell, N. J., & Eichenbaum, H.  
666 (2009). Theta-gamma coupling increases during the learning of item-context  
667 associations. *Proceedings of the National Academy of Sciences of the United  
668 States of America*, 106(49), 20942–20947.  
669 <https://doi.org/10.1073/pnas.0911331106>

670 Tosato, T., Rohenkohl, G., Dowdall, J. R., & Fries, P. (2022). Quantifying rhythmicity  
671 in perceptual reports. *NeuroImage*, 262, 119561.  
672 <https://doi.org/10.1016/j.neuroimage.2022.119561>

673 VanRullen, R. (2016). Perceptual Cycles. *Trends in Cognitive Sciences*, 20(10), 723–  
674 735. <https://doi.org/10.1016/j.tics.2016.07.006>

675 Volland, A. Z., Gardner, R. J., Moser, M.-B., & Moser, E. I. (2024). *Left-right-alternating  
676 theta sweeps in the entorhinal-hippocampal spatial map* (p.  
677 2024.05.16.594473). bioRxiv. <https://doi.org/10.1101/2024.05.16.594473>

678 Weber, J., Solbakk, A.-K., Blenkmann, A. O., Llorens, A., Funderud, I., Leske, S.,  
679 Larsson, P. G., Ivanovic, J., Knight, R. T., Endestad, T., & Helfrich, R. F. (2024).  
680 Ramping dynamics and theta oscillations reflect dissociable signatures during  
681 rule-guided human behavior. *Nature Communications*, 15(1), 637.  
682 <https://doi.org/10.1038/s41467-023-44571-7>

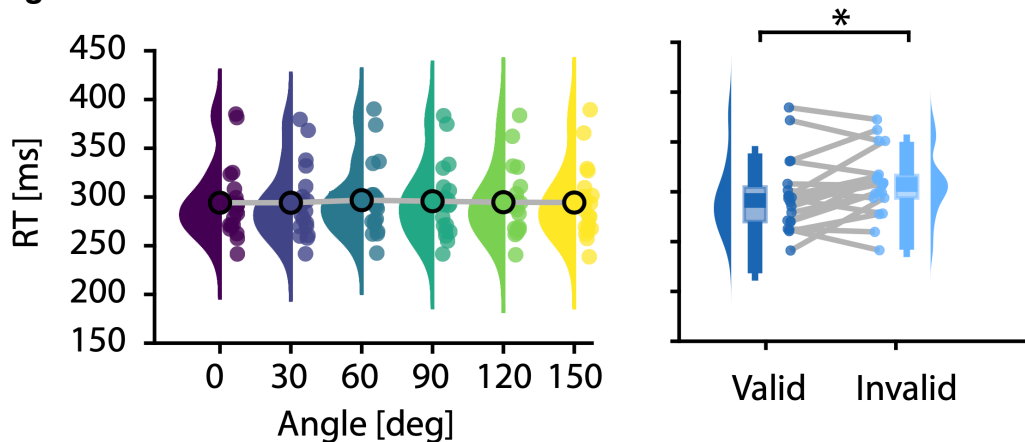
683 Wilming, N., König, P., König, S., & Buffalo, E. A. (2018). Entorhinal cortex receptive  
684 fields are modulated by spatial attention, even without movement. *eLife*, 7, 1–  
685 16. <https://doi.org/10.7554/eLife.31745>

686

687 **Supplementary Material**

688

689 **Figure S1**



690

691 **Behavioral effect of attention**

692 Left: Grand-average reaction times (RT) across subjects did not differ significantly across the six  
693 different bar orientations ( $p = 0.99$ , RM-ANOVA). Right: Average reaction times across subjects were  
694 significantly faster for validly cued (left) compared to invalidly cued targets (right,  $p = 0.03$ , Wilcoxon  
695 ranked sum test).